Optimization of Flanged Diffuser for Small-Scale Wind Power Applications

Mostafa Radwan Behery[1], Djamal Hissein Didane[2,*] Bukhari Manshoor[2]

[1] Faculty of Mechanical and Manufacturing Engineering, University Tun Hussein Onn Malaysia, 86400 Parit Raja, Batu Pahat, Johor, Malaysia
[2] Center for Energy and Industrial Environment Studies (CEIES), Faculty of Mechanical and Manufacturing Engineering, Universiti Tun Hussein Onn Malaysia, Malaysia

ARTICLE INFO	ABSTRACT
  	The development of renewable and clean energy has become more crucial to societies due to the increasing energy demand and fast depletion of fossil fuels. A state-of-the-art design for an augmented wind turbine has been introduced in the past years to increase the efficiency of compact horizontal axis wind turbines, exceeding the ideal Betz's limit of the maximum energy captured from the wind. The optimization of the flanged diffuser - so-called diffuser augmented wind turbine DAWT - is investigated numerically using the multi-objective genetic algorithm "MOGA". A 2D computational model is developed using ICEM CFD and solved by ANSYS Fluent. The Turbulence model selected is shear stress transport K-omega, with a pressure-based solver and a coupled algorithm scheme. The optimization objectives are to maximize the velocity ratio at the shroud throat and minimize shroud form dimensions. 517 design points were solved, and the design dimensions were categorized into four types: compact, small, medium, and large design. The results showed that the diffuser dimensions are the main parameters to increase velocity inside the shroud throat, where a long diffuser with a low converging angle drags more air inside the shroud, reaching in some cases more than double the upwind velocity. While the nozzle and flange are also effective in the different design types. It was found that a super long diffuser with a length ratio of 2.9 L_D to throat diameter D is optimal with a diverging angle of 7.6°, accompanied by a nozzle of ratio 1.2 L_N/D and 12.6° converging angle and a flange length ratio of 0.6 L_F/D. This optimal design increased the velocity ratio by almost 2.5 times.

1. Introduction

The possession of an energy surplus is a requisite for any kind of civilization. Increasing global population and economic production put pressure on the earth's finite resources and ecosystem capacity, pushing governments to highly consider energy resource efficiency [1]. But it also relates to the environmental impacts that result from extracting resources from natural systems, creating waste, and emitting pollutants. All these concerns are driving the world to rethink its energy mix and develop diverse sources of energy from domestic resources that can be cost-effective and replaced or renewed without contributing to climate change or major adverse environmental impacts. Primary energy sources take many forms, including fossil energy, like oil, coal and natural gas, nuclear energy,

* *Corresponding author.*
E-mail address: djamal@uthm.edu.my (Djamal Hissein Didane)

and renewable sources like solar, wind, hydropower and geothermal. They can be used directly or transformed into electricity which is another form of energy that can be carried to households and businesses through power line infrastructure [2].

Wind energy is one of the world's most old and abundant renewable energy sources, and due to its preference over other energy resources, it has been targeted for centuries [2]. Basically, wind energy converters are classified into horizontal-axis and vertical-axis wind turbines. HAWTs, or horizontal axis wind turbines, are currently the most used type of wind turbine. These turbines use aerodynamic blades, typically three blades, consisting of tapered and twisted aerofoil sections, the blades are connected to a rotor and as wind drives the rotor to turn, a shaft attached to the rotor spins a generator, the generator converts the rotating mechanical energy into electricity. Today's modern horizontal axis wind turbines have scaled up in size to multi-megawatt power ratings.

Moreover, vertical axis wind turbines are the oldest form of wind turbines. According to historical data and regardless of the use of wind in sailing, the Persians used vertical form of windmills to crush grains and pump water [3]. Despite being the oldest form of wind turbine, vertical axis wind turbine (VAWT) is still considered a niche market product, they have mainly two distinctive designs with different working principles: Darrieus and Savonious. Darrieus turbines have long, curved wings with each end attached to the top and bottom of a vertical rotor shaft that depends on lift force to spin, while Savonius wind turbines have blades built around the vertical shaft in a helix form shaped like scoops, and the differential drag causes the rotor to spin. The usage of VAWT is limited due to several reasons, most likely, low efficiency compared to HAWT, starting difficulties in Darrieus wind turbine, and relatively high vibration and noise due to installation limitations [4, 5]. Wind energy has enough power to generate electric power and it also has preference over other energy resources due to their advantages. Environmental changes can affect wind power generation; a decline in wind speeds would reduce energy yield. Wind speeds may decline due to climate change, increased forest growth, or wind farms' shadowing effect [6].

A lot of research was performed to improve the performance of horizontal-axis wind turbines. The conventional technique is improving rotor blade design where the blade is the most important part of a wind turbine, by increasing the coefficient of lift or reducing the drag coefficient [7, 8]. Large Scale Wind Turbines have been extensively examined but very few studies have been conducted on small-scale wind turbines, especially for applications near ground level at low wind speed, where VAWTs appear to be particularly promising for such conditions regardless of their operating disadvantages [9]. As a result, the introduction of a new wind power system that produces higher power output even in areas with lower wind speeds and more complex wind patterns is highly desirable. It can be also a standalone energy converter to reduce the dependency on the national grid [10]. Furthermore, small-scale wind turbines have low efficiency due to the small swept area by blades and low wind speeds as the power in the wind is directly proportional to the cubic power of the velocity of the wind. Therefore, increasing the mass flow rate affecting the turbine's blade should significantly increase wind power generation [11].

One of the methods to improve the performance of small-scale wind turbines by increasing the wind speed approaching the wind turbine is the so-called Diffuser-Augmented Wind-Turbine (DAWT), sometimes called a shrouded or ducted wind turbine. It is basically a turbine installed inside a cone-shaped structure, where this technique of augmenting air simply increases the upstream wind speed of the turbine by generating separation regions behind it, where low-pressure areas appear to draw more air through the rotors compared to a bare wind turbine, a flanged diffuser form surrounding a vertical axis wind turbine is one of the popular configuration adopting the idea of wind augmentation using a diffuser structure and thus increasing the overall power output of the wind turbine, exceeding the ideal Betz's limit of the maximum energy captured from the wind [12].

Betz was the first to discover the potential of ducted/diffuser wind turbines, as claimed by Hoopen [13], Sanuki [14] conducted experiments on a tiny wind turbine with and without a shroud. He found that the power coefficient of the shrouded turbine with three blades rose by 4% in comparison to the identical turbine without a shroud, showing a 30% improvement in shrouded turbine performance [14]. The idea was proposed again by Lilley *et al.,* [15] that a good shroud design is capable of increasing output by 65% compared to an unshrouded wind turbine. The idea of fabricating the diffuser using light fiberglass was also suggested [16–18]. Preformed experimental studies showed that power extraction beyond the Betz limit is achievable. However, DAWT technology is considered not profitable since its costs outweigh its revenues when compared to relative conventional wind turbines. Thus, these experiments were discontinued. Thus, CFD studies of blade and shroud design were carried out. The DAWT design and performance were optimized by Phillips [19]. The results of the optimization concluded that the data of the full-scale DAWT showed that only an augmentation level of 2.4 instead of the expected 9 was reached. This was also supported in other publications. A numerical investigation was carried out by Abe *et al.,* [11] for the flow fields of a small wind turbine with a flanged diffuser. The formation of vortices creates a low-pressure region drawing more mass flow to the turbine inside the shroud. An experimental model in the same publication resulted in a power coefficient higher than the Betz limit (=16/27) due to the flanged diffuser effect.

Ohya *et al.,* [20] continued this study experimentally, a wind turbine system that consists of a diffuser with a broad-ring flange at the exit. The power augmentation of this investigation was increased by a factor of around 4 to 5 in comparison to the bare wind turbine. These results were verified through field measurements in addition to wind tunnel experiments. In 2010, this research was extended by the same authors for further field experiments and different compact brimmed diffuser shapes for the so-called wind lens and it showed a two to threefold increase in the output power as compared to the conventional bare wind turbine [21]. The shape and geometry of the diffuser, the airfoils of the blades, and the wind speed at the mounting point all affect how well a diffuser-augmented Wind Turbine performs. The primary factors influencing this wind energy device's aerodynamic performance are its geometric elements. The diameter of the inflow diffuser is affected by the rotor diameter, diffuser length, diffuser angle, and brim height (flange height) [22, 23].

Several optimization studies took place to identify the optimum configuration for the diffuser shroud. Liu [24] combined genetic algorithm and CFD as an effective way for optimizing wind lens profiles. The shape of the wind lens was optimized using MOGA performed by Khamlaj [25], The optimization results showed a power increase of 12-14% in compact designs. A sensitivity analysis for the angle and length of the diffuser in addition to the brim height was studied by Maw [26] using numerical simulations, where he concluded that a diffuser length of L/D = 1, brim height is H/D = 0.35 and a converging angle equals to 10° can achieve nearly 50% higher performance than that of baseline diffuser design used in his previous research in which a 25% increase in performance was reported. It was also mentioned that if the diffuser length is too long, the maximum length studied was L/D = 1.5, which will decrease the performance of the wind turbine. On the contrary, A. Elsayed [21] mentioned in his numerical parametric study that a long diffuser (L/D=3.94) with an open angle of 5.47 and flange height (h/D=0.29) can maximize the diffuser entrance average velocity ratio to 1.763. Using a Simplex algorithm in a wide search space and the same design variables used in Maw's work [26]. He also stated that power output can be augmented by a factor of 2.76:5.26 compared to bare wind turbines.

To Summarize the literature of the previous studies, the potential of installing wind turbines in urban areas is still very challenging. Diffuser technologies have received several developments and

evolutions to understand the phenomena that enhance the flow fields around the shroud device, and consequently increase wind turbine-produced output, which can be a solution for applications near ground level. Different configurations of the shroud profile were investigated including a simple diffuser, a diffuser accompanied with an inlet nozzle, a flanged diffuser, a curved diffuser, and a multilayer diffuser. Optimization techniques were used to evaluate the best design parameters in terms of size in parallel with the velocity augmentation. Those investigations showed that the velocity augmentation is limited to 1.5 to 1.7, and this is one of the reasons that small wind turbines are still far from technological maturity and economic competitiveness [27]. In some studies that extended this parameter to include long diffusers as Elsayed [28], the velocity ratio can be multiplied by 2 to 2.5 of the inlet velocity.

The work presented in this paper is an extension to those optimization studies aiming to investigate different forms of the shroud dimension while considering the inlet opening (nozzle) by designing an optimization loop with embedded CFD numeral simulations to find the optimal dimensions. While this study is an optimization process on different empty shroud numerical models, it derives the optimal dimensions of the diffuser geometry including the converging section, diverging section, and the flange, that can develop the highest velocity ratio when affecting the blades of a turbine. The optimization study also provides design guidance by analyzing a wide range of numerical models in a large search space to evaluate the best design parameters in terms of size in parallel with the velocity augmentation as the diffuser makes the wind turbine quite bulky, increasing the overall aerodynamic drag and thus a stronger mounting will be required through minimizing the diffuser geometry as possible.

2. Methodology

A fully automatic optimization takes place, using the mode FRONTIER commercial program. The optimization loop model was created and MOGA II was applied to solve this model coupled with CFD. The two objectives of the optimizer were to maximize the average velocity ratio inside the Shroud Throat and to minimize shroud dimensions.

2.1 The Turbulent Models

As a CFD-based optimization was selected for this research, the prerequisite for CFD modeling is the setup of governing equations; the three fundamental governing equations are the conservation of mass, momentum, and energy. After that, a mesh is made, and boundary conditions are chosen based on various flow conditions. The purpose of the meshing model is to discretize equations and boundary conditions into a single grid. A cell is a basic element in a structured or unstructured grid. The basic elements of a two-dimensional unstructured grid are triangular and quadrilateral cells.

To create a two-dimensional model ICEM CFD was used, and it was used also to create a structured mesh for the shroud. CFD simulation was done for flow fields inside using the RANS model as a governing equation. The equation of Reynolds-averaged Navier-Stokes (RANS) is defined as:

$$\rho \frac{DU_i}{Dt} = \frac{\partial P}{\partial X_i} + \frac{\partial}{\partial X_i}\left[\mu\left(\frac{\partial U_i}{\partial X_j} + \frac{\partial U_j}{\partial U_i}\right) - \rho\overline{\acute{u}_i\acute{u}_j}\right] \tag{1}$$

Shear-stress transport (SST) k-ω model was also selected because it absorbs the property of good accuracy in the near-wall region of the standard k-ω model and good precision in the far field region

of the k−ε model. Consequently, compared to the traditional k-ω model, it is more accurate and trustworthy for a wider class flow.
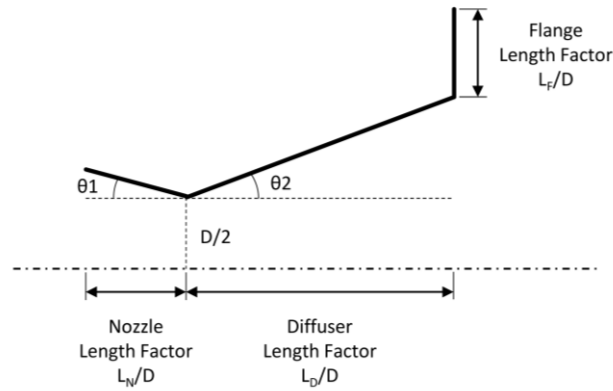
2.2 Optimization

Optimization Algorithms are more adaptable to dealing with issues involving complex objective functions and limitations. For this reason, these procedures are now more suited for use in industrial settings. Evolutionary Algorithms (EA) are considered stochastic methods designed to tackle complex problems. Within an EA, a group of artificial beings explores the problem's domain, aiming to uncover the most optimal regions within the search space [29].

Multi-objective genetic algorithm (MOGA) is a direct search method for multi-objective optimization problems. It is based on the process of the genetic algorithm; the population-based property of the genetic algorithm is well applied in MOGAs. By comparing it with the traditional multi-objective algorithm whose aim is to find a single Pareto solution, the MOGA intends to identify numbers of Pareto solutions. During the process of solving multi-objective optimization problems using a genetic algorithm, one needs to consider the elitism and diversity of solutions. However, there are some trade-offs between elitism and diversity. For some multi-objective problems, elitism and diversity are conflicting with each other. Therefore, solutions obtained by applying MOGAs have to be balanced with respect to elitism and diversity. In this paper, the proposed method was already tested by some well-known benchmarks and compared its numerical performance with other MOGAs; the result shows that the proposed method is efficient and robust [30]. The Genetic Algorithms for multi-objective optimization can find difficulties in converging to the true Pareto frontier and can get stuck in a local Pareto front. A new elitism operator MOGA II that uses a smart multi-search elitism can preserve some excellent solutions without bringing premature convergence into local optimal fronts. Moreover, the efficiency of this algorithm will be orderly proved on six well-known test functions for multi-objective optimization [31, 32].

2.2.1 Optimization parameters

The nozzle and the diffuser as well as the flange are the components of the shroud design in this research. All sizes are presented as a ratio to shroud throat diameter to keep all design parameters in a dimensionless form except the opening angle of the nozzle and the diverging angle of the diffuser (See Figure 1). The Optimization parameters that need to be investigated in this research as shown in Figure 1 are:

i.   Nozzle length factor L_N/D
ii.   Diffuser length factor L_D/D
iii.   Flange length factor L_F/D
iv.   Converging angle (Nozzle) θ_1
v.   Diverging angle (Diffuser) θ_2

Fig. 1. Optimization parameters

For optimization parameters, Table 1 shows the selected spatial parameters for geometric variables. The nozzle was set to have a minimum length of 0.1 LN/D that can be increased to two times the turbine throat, the flange also was selected to be within the same range, while the diffuser was increased to three times the shroud throat. Both the converging angle of the nozzle and the diverging angle of the diffuser were set to have the same range starting from 0.1˚ to 40˚. All the design parameters have a wide design space as the DOE step was set to 0.1.

Table 1
Range of the design parameters

Optimization parameter	Minimum allowed value	Maximum allowed value	Step
Nozzle length factor L_N/D	0.1	2	0.1
Diffuser length factor L_D/D	0.1	3	0.1
Flange length factor L_F/D	0	2	0.1
Converging angle (Nozzle) θ_1	0.1˚	40˚	0.1˚
Diverging angle (Diffuser) θ_2	0.1˚	40˚	0.1˚

2.3 Grid Generation

To create a two-dimensional model, ICEM CFD was used, and it was used also to create a structured mesh for the shroud (see Figure 2), and boundary conditions were chosen based on various flow conditions. In order to get a good and structured mesh to ease computational simulations, a TCL (scripting language) code was created to cover all design points in the selected search space and to cover different design parameters without affecting mesh quality, taking advantage of the domain blocking options in ICEM CFD to create a structured mesh with an adequate number of near-wall cell in order to meet wall function and Y+ requirements.
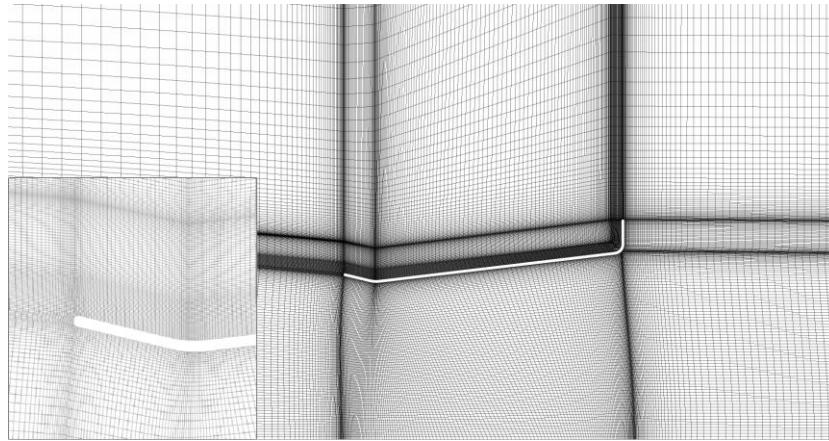
Fig. 2. Mesh quality of the current

2.4 Numerical Methods

The numerical calculation was pressure-based through steady flow simulations. Pressure-velocity coupling was adopted, as using a pressure-based coupled algorithm has some advantages compared to segregated algorithms making it more efficient and robust in steady-state flow calculations. Boundary conditions are shown in Figure 3. For the inlet, a 3 m/s constant free stream with turbulent intensity of 3% was predefined. For top and bottom boundaries, symmetry and axis conditions were prescribed respectively. For the flow outlet, a pressure outlet with 5% backflow turbulence was selected.

The convergence criteria were set to 10^{-5} while the max no. of iterations was 300 to avoid unnecessary computing costs, to obtain precise results and to be able to investigate the flow fields and pressure distributions accurately.
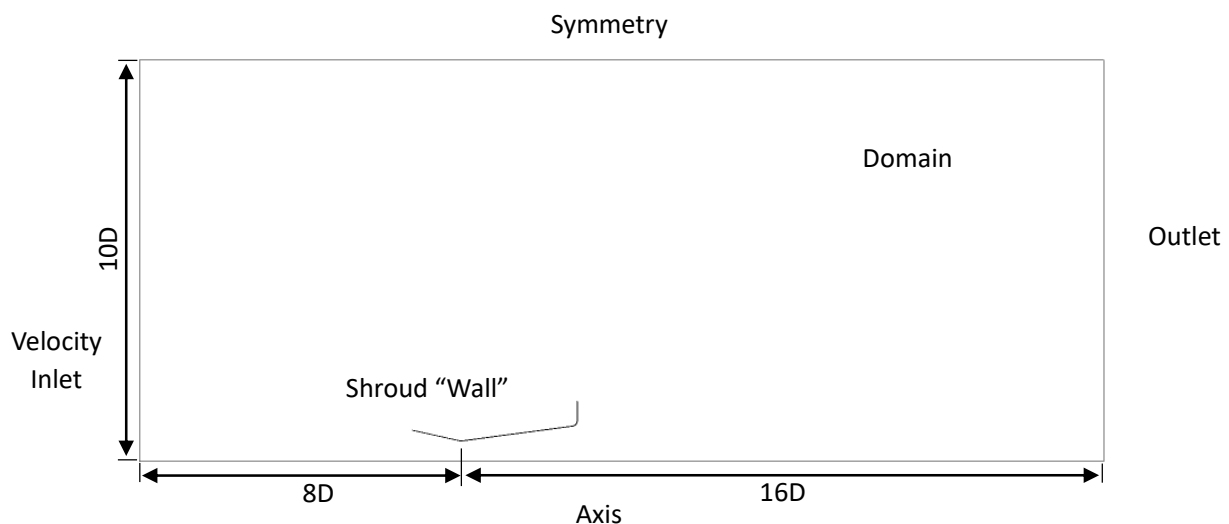

Fig. 3. Computational and boundary conditions

3. Results
3.1 Numerical Case Validation

Wind velocity distributions on the shroud's central axis are compared with the available experimental measurements of Ohya [11]; a circular-diffuser model with a flange, diffuser factor L_D/D

= 1.5, Diverging Angle (Diffuser) θ2 = 4˚, Flange Factor L_F/D = 0.625, as seen in Figure 4. These results give a good agreement obtained between experiments and the present CFD model using the shear-stress transport (SST) k-ω model. The overall error is limited to 4% on average, the velocity ratio in the shroud throat showed almost no variations where this research is focusing on. The simulated velocity ratio is within the scatter of the available experimental data.
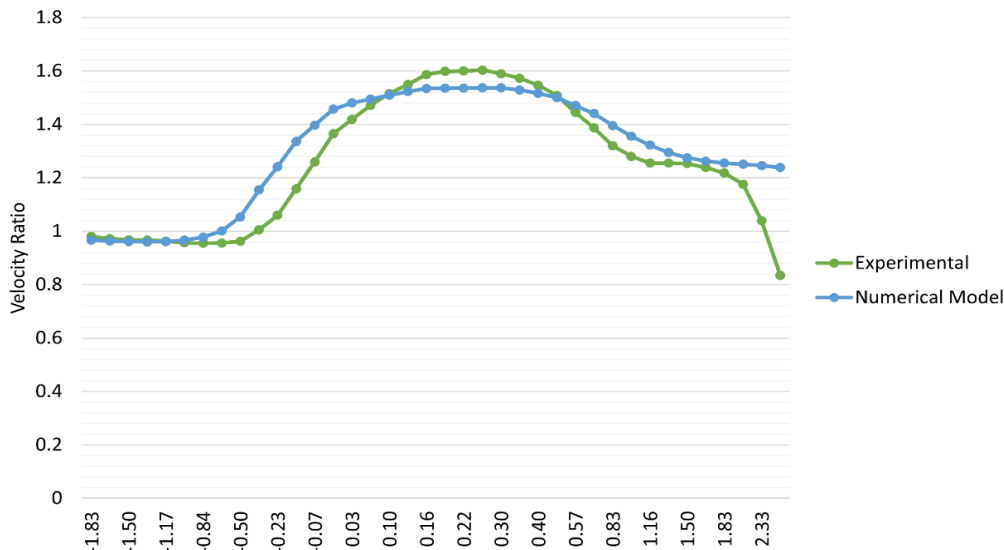

Fig. 4. Comparison of the present numerical model with previous experimental results

3.2 Optimization Results

In order to understand optimization results, the mechanism of the MOGA II needs to be first demonstrated. The ability to prevent premature convergence and approximate the set of optimal trade-offs in a single run promotes its usage to achieve fast Pareto convergence. The tendency of the optimization iterations to have retained design cases in new populations is clearly recognized to stabilize optimization convergence. The maximum number of iterations was 300 to avoid unnecessary computing costs. This was the main reason non-converged design cases were excluded in the discussion of the results regardless of their substantial proportion which is close to 23% of solved cases.

3.2.1 Factor analysis

In Figure 5, the five parameters selected for the optimization model are represented in a sequence of box-whisker plots (sometimes called the design of experiments plot) to determine a ranking list of the important factors and the most appropriate value for each factor. In order to determine whether the mean value is increasing or decreasing, all input factors are shown in two levels, "high" (or simply "+") and "low" (or simply "-") where the data set is split into two equal-sized groups. Figure 6 shows a parallel coordinate chart for the design parameters to have a better visualization of their effect on the first objective of the optimization loop. As shown in Figure 5 and Figure 6, the diffuser length is the most important factor for the design of the shroud, other factors affect the optimization objective, it can be noticed that the optimal shape most likely has a long diffuser with a low converging angle, a short nozzle with medium or large opening angle, while a short flange has a moderate effect in some cases.
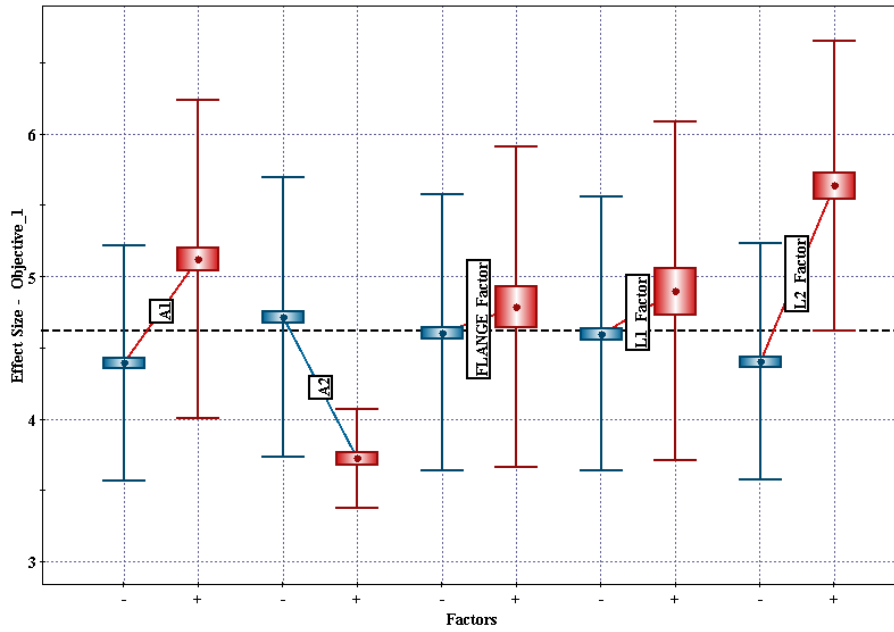
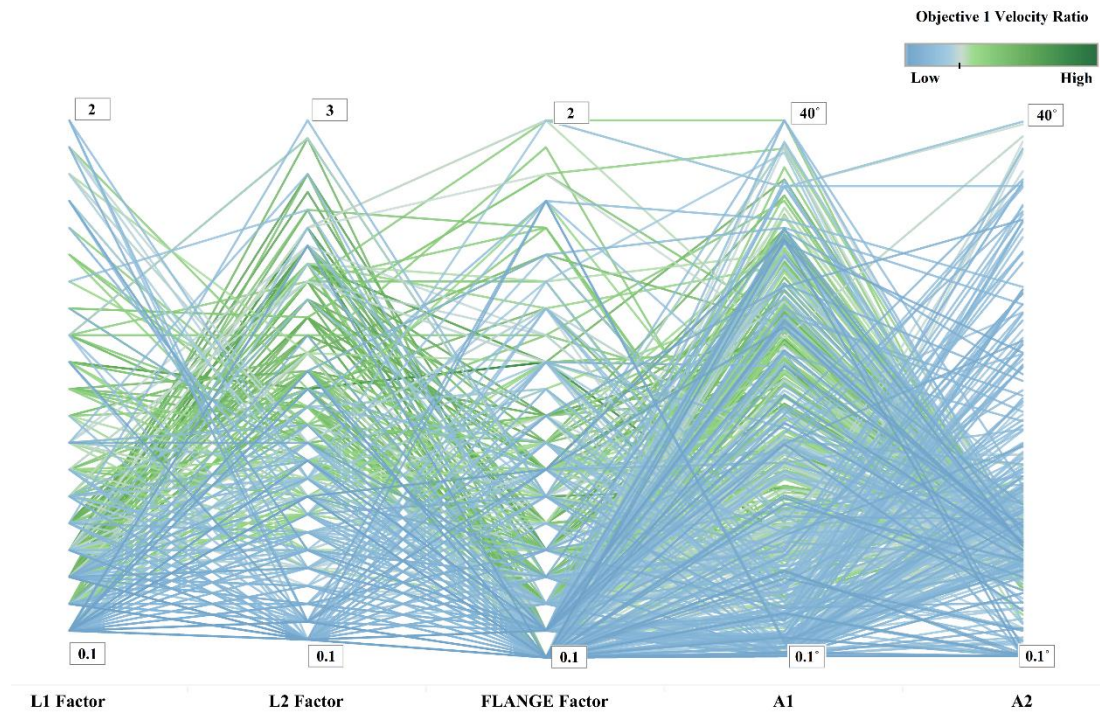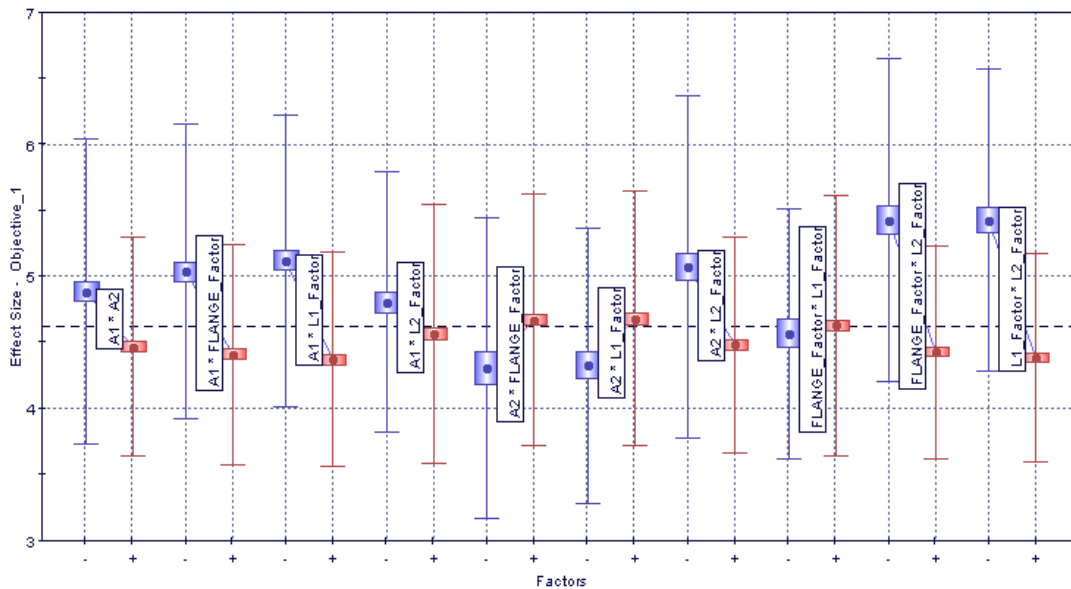**Fig. 5.** Main effects chart for optimization parameters

Fig. 6. Parallel coordinates chart for optimization parameters

In Figure 7, the main effects chart is extended to display the first-order interaction effects for determining a ranking list of the most significant interaction between each parameter involved, each box plot shows if the mean varies in the two groups of data, where a large difference implies the interaction is important and a small difference would imply the opposite It is clearly observed in Figure 6 that the diffuser length and the flange length is the most significant interaction, both the interaction between the diffuser length and its diverging angle and the interaction between the

nozzle length and its opening angle is also important, in addition to the interaction between the nozzle and diffuser length.


Fig. 7. Interactions effects chart for the first optimization objective: maximizing velocity ratio inside the shroud throat

In order to have a deep investigation of each parameter and how it affects the optimization objectives, mainly the first objective, some cases were selected to see the absolute effect of changing the value of this parameter while the others remained constant, starting with the diffuser length L_D, as shown in Figure 8, a comparison between two design cases was done, the first one has a medium-sized diffuser ($L_D = 0.8$) and the second one with a compact diffuser ($L_D = 0.1$), same for the nozzle and the flange. The effect of the diffuser length on the velocity contours is obvious, despite both designs forming wakes at the end of the geometry, two recirculation zones with the same size, the first one drags air at a higher speed as shown.

The effect of the opening angle of the nozzle on the optimization objective can be seen in Figure 9, two large-sized shrouds were selected where one has an opening angle of 12.6° and the other is 38.5°, increasing the opening angle in the second design point results in moving the recirculation zone from the end of the shroud geometry to the outside part of the geometry above the nozzle and shroud, the velocity ratio drops from 2.43 to 1.74. For the effect of diffuser diverging angle, it can be easily determined from different design points that increasing the diverging angle makes the wake zone start from the shroud throat and hence the area swept by the incoming air stream remains constant leading to a slight increase in the velocity ratio compared to other design point having a smaller diverging angle.
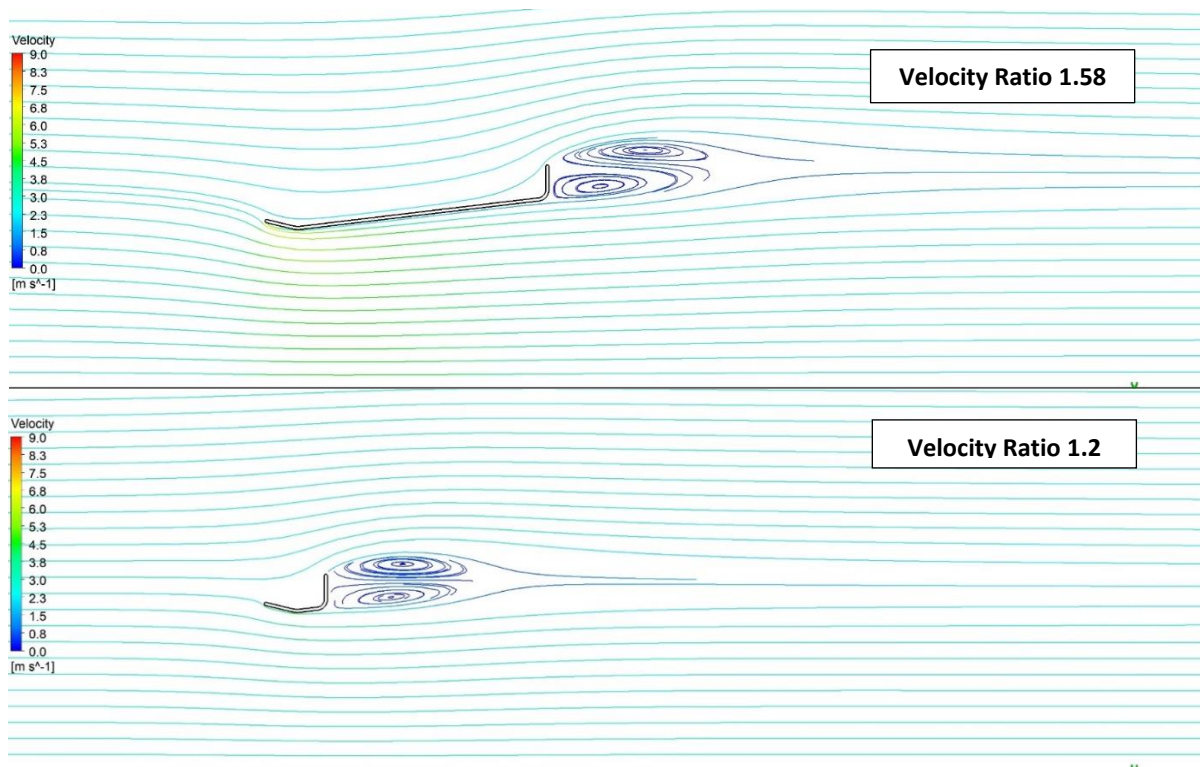
Fig. 8. Effect of diffuser length L_D on velocity streamlines and downstream vortices
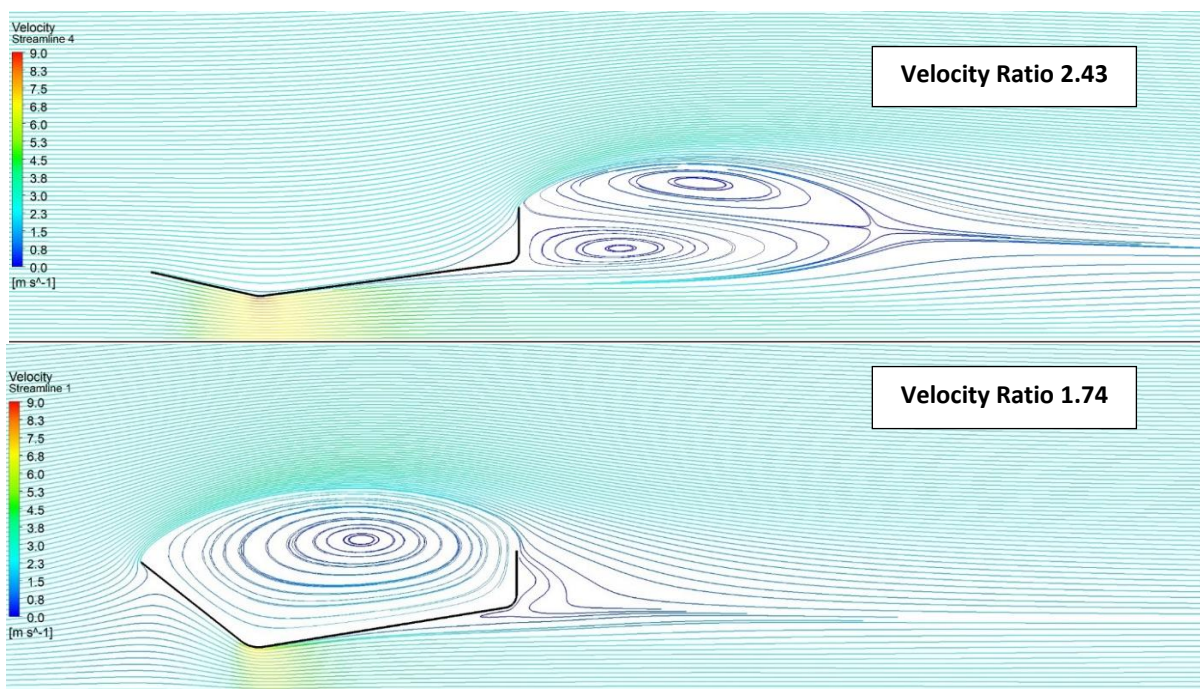
Fig. 9. Effect of opening angle of nozzle A_1 on velocity streamlines and downstream vortices

While most of the optimal shapes in large design points have a significant nozzle, the length of the nozzle L_N seems to have a minor effect on the flow regime around the shroud geometry. As shown in Figure 10, increasing the size of the nozzle does not affect a poor-performance shroud.

It can be observed from Figure 11 and Figure 12 The effect of the flange on the shroud performance. In Figure 11, a large flange increased the velocity ratio by almost 20%, and the large recirculation zone formed at the geometry is clear to have a positive effect. While in Figure 12, the

flange doesn't improve the velocity ratio despite the formation of the recirculation zone, but in this case, the large diverging angle of the diffuser pulled these wakes to be close to the geometry center and the laminar flow regime has almost the same area across the shroud. The added flange has no effect on the velocity streamlines in this case.
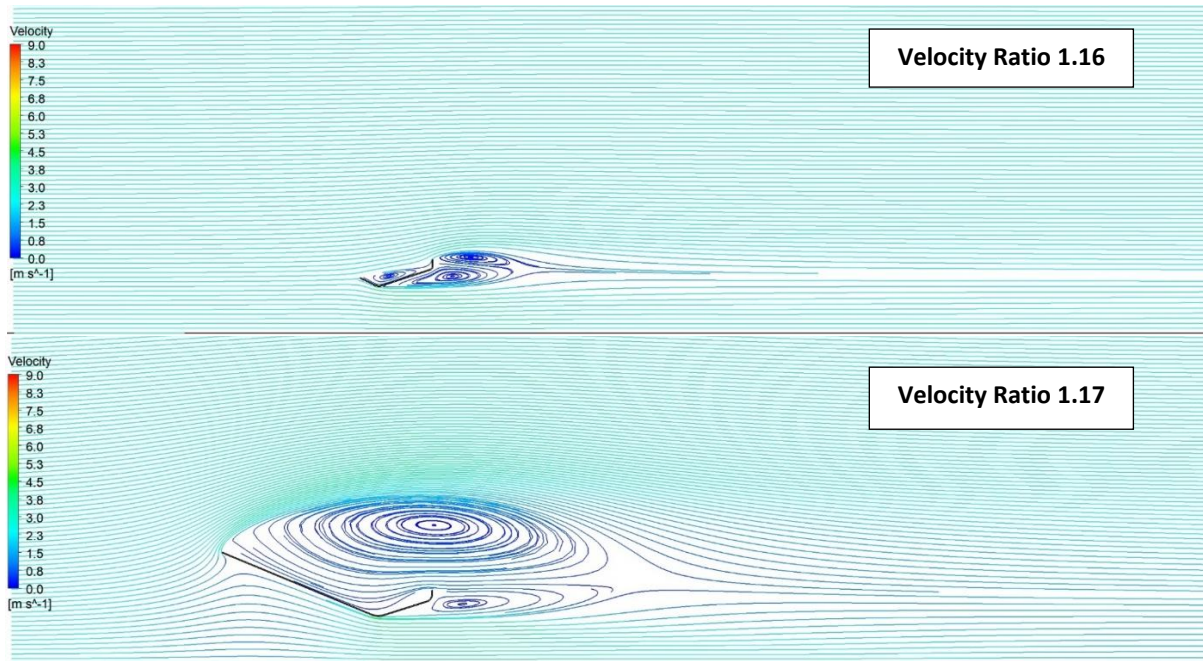

Fig. 10. Effect of nozzle length LN on velocity streamlines and downstream vortices
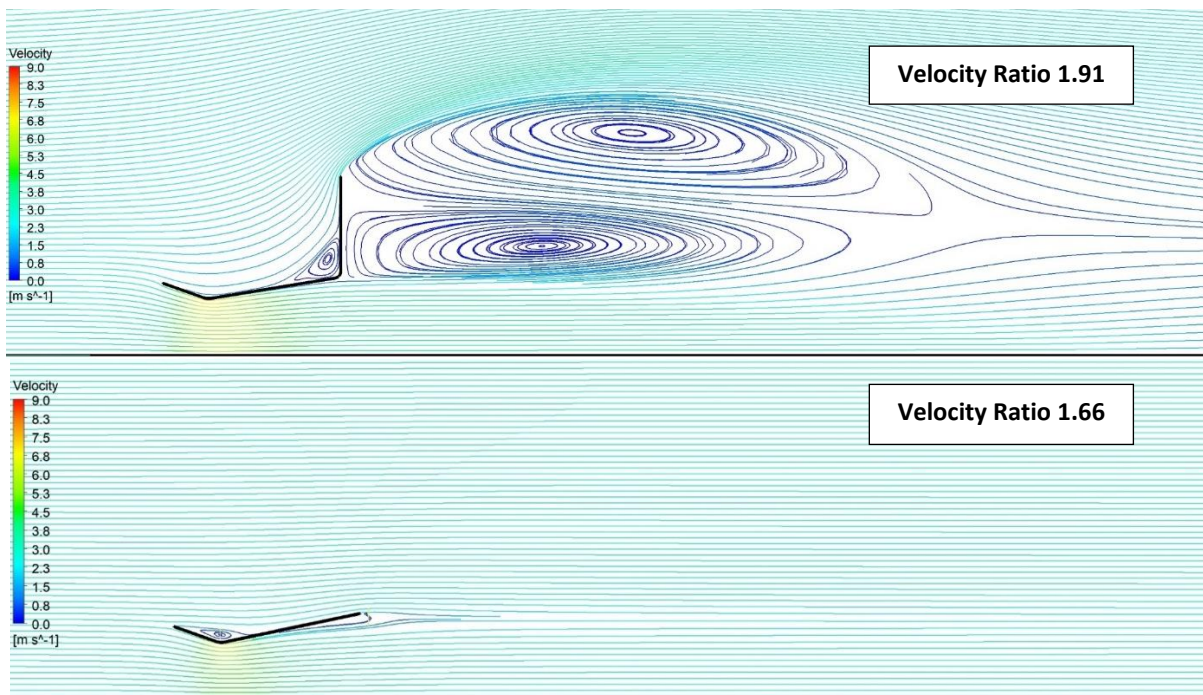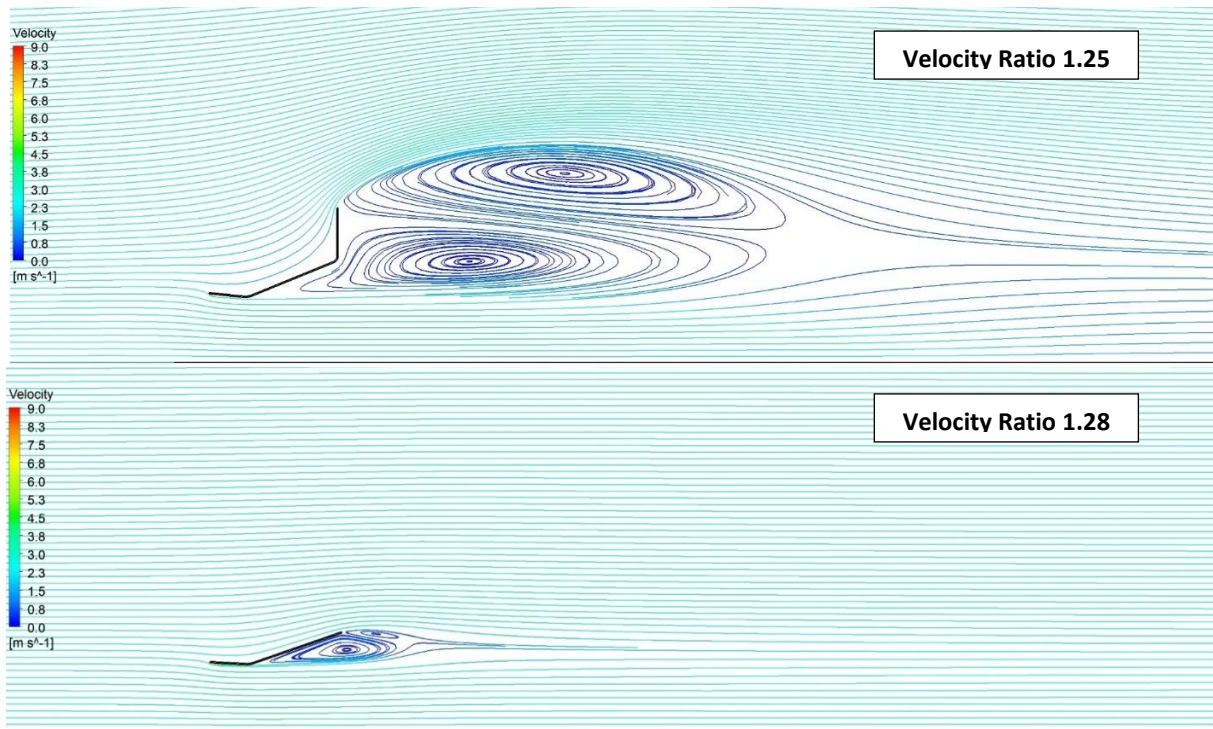

Fig. 11. Effect of flange L_F on velocity streamlines and downstream vortices

Fig. 12. Effect of flange L_F on velocity streamlines and downstream vortices

3.2.2 Optimal design

To be able to identify the effect of design parameters on the optimization objectives, mainly the first objective, the shroud design was divided into four categories according to the overall size of the formed Duct:

i.   Compact Design $(L_N/D + L_D/D + L_F/D) < 0.3$
ii. Small Design $0.3 < (L_N/D + L_D/D + L_F/D) < 0.6$
iii. Medium Design $0.6 < (L_N/D + L_D/D + L_F/D) < 1.2$
iv. Large Design $1.2 < (L_N/D + L_D/D + L_F/D)$

Table 2 shows the number of each design point solved per category as well as the Optimal design configuration of the optimal design point.

**Table 2**
Optimal design point in each category

		Compact design	Small design	Medium design	Large design
No. of design points in the optimization		49	60	177	386
No. of design points solved		32	43	126	316
Dimensions of optimum design point DP	Nozzle length factor L_N/D	0.1	0.1	0.1	1.2
	Diffuser length factor L_D/D	0.1	0.4	1	2.9
	Flange length factor L_F/D	0.1	0.1	0.1	0.6
	Converging angle (Nozzle) θ_1	1.4°	29.1°	31.6°	12.6°
	Diverging angle (Diffuser) θ_2	0.3°	9.4°	8.4°	7.6°
Velocity ratio at shroud throat		1.22	1.44	1.76	2.43

The optimal design for the compact design category achieved an average velocity of 1.22 m/s inside the shroud throat. As shown in Figure 13, the velocity contours and velocity path lines show medium-sized recirculation zones behind the flange where the pressure drops allowing more air to flow inside the shroud.
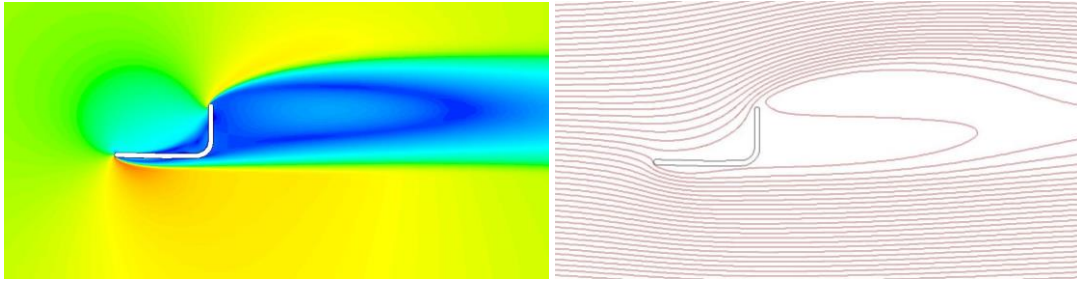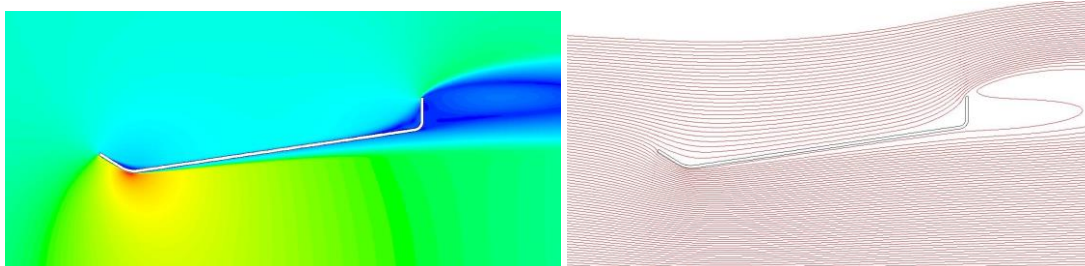

Fig. 13. Velocity contours and path lines around the shroud profile of the optimal design point in the compact size category

In the second category, small design, the optimal design achieved an average velocity of 1.44 m/s inside the shroud throat. It is obvious from Figure 14 that compared to those of the optimal design point for the compact design category, the quit larger recirculation zone in the upper downstream of the shroud geometry tends to drag more air inside, improving the velocity ratio by 15%. This zone plays the most important input for the optimization process, where the larger the recirculation zone, the higher velocity can be reached at the shroud throat. The same concept can be applied in the third category, the low diverging angle and longer diffuser results in a larger recirculation at the end of the shroud geometry and higher velocity ratio achieved (see Figure 15). It shows also a full laminar flow regime inside the diffuser, and this is a main parameter for the shroud performance. The optimal design point in the third category reached a velocity ratio of 1.76.
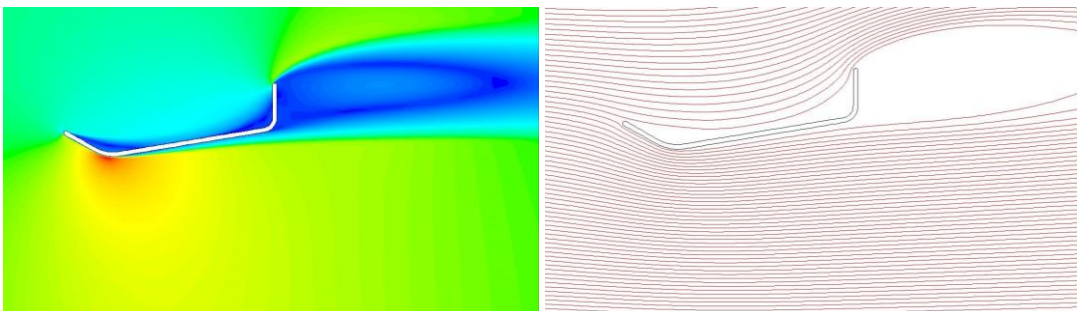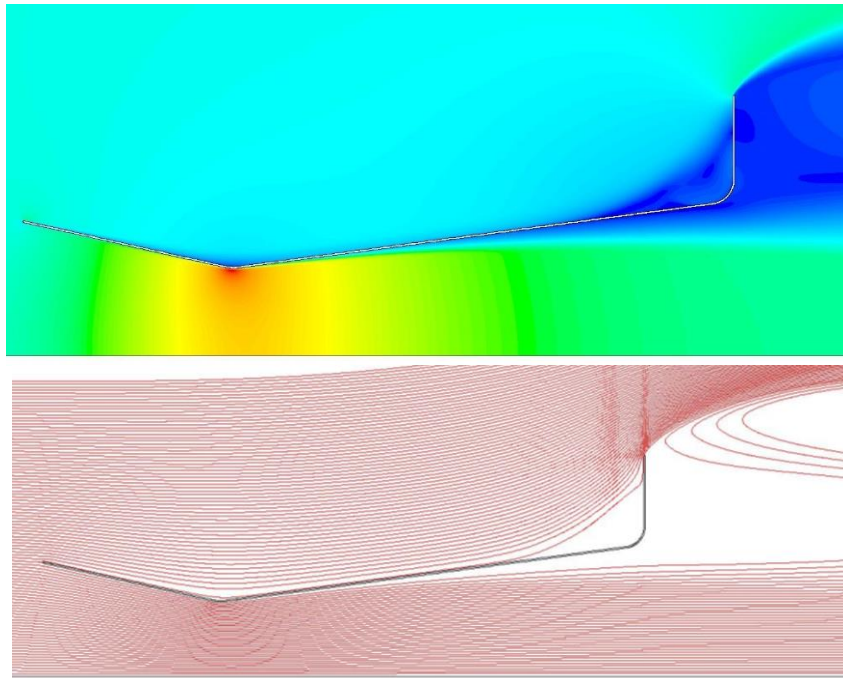

Fig. 14. Velocity contours and path lines around the shroud profile of the optimal design point in the small size category

Fig. 15. Velocity contours and path lines around the shroud profile of the optimal design point in the medium-size category

In the large design category, in which most of the optimization cases were generated by the optimizer, the optimal design for this category achieved an average velocity of 2.43 m/s inside the shroud throat (see Figure 16).

Fig. 16. Velocity contours and pathlines of the optimal design point in the large design category and the whole optimization results

As discussed previously in the factor analysis section, the main input to maximize the velocity ratio is to have a large eddy or recirculation zone at the end of the shroud while keeping flow laminar inside the shroud, the latest can be achieved by lowering the diffuser angle, it is strange that the optimal design point in this optimization model was one of the 16 cases solved in the first generation, ranked 12 of total 800 design point selected by the optimizer. This can be due to the combination of long diffuser, low diverging angle and flange, as most cases with this criterion have a velocity ratio ranging from 2 to 2.43. This is also an indication that a longer diffuser can achieve higher velocity ratios, but this should be investigated experimentally as well to check the behavior of the flow fields in the downstream region where backflow may occur.

4. Conclusion

In this work, numerical simulations were performed on a different design of an empty flanged diffuser with a concentrator (nozzle) through a random-based optimization loop. The conclusion and outcomes of this research can be summarized in the following points:

i.   The CFD numerical model results for the diffuser shroud have shown good agreement with the published experimental measurements of the velocity distribution on the central ais of an empty flanged diffuser. The simulated velocity ratio using the realizable k-ω model is within the scatter of the available experimental data. Therefore, this turbulence model was used for the investigation of multiple design points.

ii.   ICEM CFD script file was developed to create the geometry domain and mesh for a wide range of design parameters, using the previously mentioned turbulence model and configuration used in the validated numerical case.

iii.   The Genetic Algorithm model was a good choice that makes the optimization parameters come across a wide range of design cases, some of which seem awkward, but it helps to know how the design parameters selected in this study affect velocity augmentation.

iv.   It was found that a super long diffuser with a length ratio of 2.9 LD to throat diameter D is optimal with a diverging angle of 7.6˚, accompanied by a nozzle of ratio 1.2 LN/D and 12.6˚ converging angle and a flange length ratio of 0.6 LF/D. This optimal design increased the velocity ratio by almost 2.5 times.

v.   The results showed that the diffuser dimensions are the main parameters to increase velocity inside the shroud throat, where a long diffuser with a low converging angle drags more air inside the shroud, reaching in some cases more than double the upwind velocity. While the nozzle and flange are also effective in the different design types.

Acknowledgement

References

[1]   Didane, Djamal Hissein, Abas Ab Wahab, S. Shamsudin, and N. Sand Rosly. "Wind as a sustainable alternative energy source in Malaysia-a review." *ARPN Journal of Engineering and Applied Sciences* 11, no. 10 (2016): 6442-6449.

[2]   Hau, Erich. *Wind turbines: fundamentals, technologies, application, economics*. Springer Science & Business Media, 2013.https://doi.org/10.1007/978-3-642-27151-9

[3]   J. G. Mcgowan and J. F. Manwell, Wind Energy Explained. West Sussex: John Wiley & Sons Ltd, 2002.

[4]   Loutun, Mark Jason Thomas, Djamal Hissein Didane, Mohd Faizal Mohideen Batcha, Kamil Abdullah, Mas Fawzi Mohd Ali, Akmal Nizam Mohammed, and Lukmon Owolabi Afolabi. "2D cfd simulation study on the performance of various naca airfoils." *CFD Letters* 13, no. 4 (2021): 38-50.https://doi.org/10.37934/cfdl.13.4.3850

[5]   Halmy, Muhammad Syahmy Mohd, Djamal Hissein Didane, Lukmon Owolabi Afolabi, and Sami Al-Alimi. "Computational fluid dynamics (cfd) study on the effect of the number of blades on the performance of double-stage savonius rotor." *Cfd Letters* 13, no. 4 (2021): 1-10. https://doi.org/10.37934/cfdl.13.4.110

[6]   International Energy Agency. *Variability of wind power and other renewables: management options and strategies*. International Energy Agency, 2005.

[7]   Didane, D. H., Sofian Mohd, Z. Subari, Nurhayati Rosly, MF Abdul Ghafir, and MF Mohd Masrom. "An aerodynamic performance analysis of a perforated wind turbine blade." In *IOP Conference Series: Materials Science and Engineering*, vol. 160, no. 1, p. 012039. IOP Publishing, 2016. https://doi.org/10.1088/1757-899X/160/1/012039

[8]   Didane, D. H., Sofian Mohd, Z. Subari, Nurhayati Rosly, MF Abdul Ghafir, and MF Mohd Masrom. "An aerodynamic performance analysis of a perforated wind turbine blade." In *IOP Conference Series: Materials Science and Engineering*, vol. 160, no. 1, p. 012039. IOP Publishing, 2016. https://doi.org/10.1088/1757-899X/160/1/012039

[9]   Al-Ghriybah, Mohanad, Mohd Fadhli Zulkafli, Djamal Hissein Didane, and Sofian Mohd. "Performance of the savonius wind rotor with two inner blades at low tip speed ratio." *CFD Letters* 12, no. 3 (2020): 11-21. https://doi.org/10.37934/cfdl.12.3.1121

[10]   Alquraishi, Balasem Abdulameer, Nor Zelawati Asmuin, Sofian Mohd, Wisam A. Abd Al-Wahid, and Akmal Nizam Mohammed. "Review on diffuser augmented wind turbine (dawt)." *International Journal of Integrated Engineering* 11, no. 1 (2019). https://doi.org/10.30880/ijie.2019.11.01.021

[11]   Abe, Ken-ichi, and Yuji Ohya. "An investigation of flow fields around flanged diffusers using CFD." *Journal of wind engineering and industrial aerodynamics* 92, no. 3-4 (2004): 315-330. https://doi.org/10.1016/j.jweia.2003.12.003

[12]   Van Bussel, Gerard JW. "The science of making more torque from wind: Diffuser experiments and theory revisited." In *Journal of Physics: Conference Series*, vol. 75, no. 1, p. 012010. IOP Publishing, 2007. https://doi.org/10.1088/1742-6596/75/1/012010

[13] Ten Hoopen, P. D. C. "An Experimental and Computational Investigation of a Diffuser Augmented Wind Turbine: with an application of vortex generators on the diffuser trailing edge." (2009).

[14] Sanuki, M., S. Kimura, and N. Tsuda. "Studies on Biplane Wind Vanes, Ventilator Tubes. and Cup Anemometers." *Papers in Meteorology and Geophysics* 2, no. 3-4 (1951): 317-333. https://doi.org/10.2467/mripapers1950.2.3-4_317

[15] Lilley, G. M., and W. J. Rainbird. "A preliminary report on the design and performance of ducted windmills." (1956).

[16] Foreman, K. M. *Preliminary design and economic investigations of Diffuser-Augmented Wind Turbines (DAWT)*. No. SERI/TR-98073-1B. Grumman Aerospace Corp., Bethpage, NY (USA). Research Dept., 1981.https://doi.org/10.2172/5449342

[17] Gilbert, B. L., and K. M. Foreman. "Experiments with a diffuser-augmented model wind turbine." (1983): 46-53. https://doi.org/10.1115/1.3230875

[18] Igra, Ozer. "Research and development for shrouded wind turbines." *Energy Conversion and Management* 21, no. 1 (1981): 13-48. https://doi.org/10.1016/0196-8904(81)90005-4

[19] Phillips, Derek Grant. "An investigation on diffuser augmented wind turbine design." PhD diss., ResearchSpace@ Auckland, 2003.

[20] Ohya, Yuji, Takashi Karasudani, Akira Sakurai, Ken-ichi Abe, and Masahiro Inoue. "Development of a shrouded wind turbine with a flanged diffuser." *Journal of wind engineering and industrial aerodynamics* 96, no. 5 (2008): 524-539. https://doi.org/10.1016/j.jweia.2008.01.006

[21] Ohya, Yuji, and Takashi Karasudani. "A shrouded wind turbine generating high output power with wind-lens technology." *Energies* 3, no. 4 (2010): 634-649. https://doi.org/10.3390/en3040634

[22] Kosasih, Buyung, and Andrea Tondelli. "Experimental study of shrouded micro-wind turbine." *Procedia Engineering* 49 (2012): 92-98. https://doi.org/10.1016/j.proeng.2012.10.116

[23] Kishore, Ravi Anant, Thibaud Coudron, and Shashank Priya. "Small-scale wind energy portable turbine (SWEPT)." *Journal of wind engineering and industrial aerodynamics* 116 (2013): 21-31. https://doi.org/10.1016/j.jweia.2013.01.010

[24] Liu, Jie, Mengxuan Song, Kai Chen, Bingheng Wu, and Xing Zhang. "An optimization methodology for wind lens profile using computational fluid dynamics simulation." *energy* 109 (2016): 602-611. https://doi.org/10.1016/j.energy.2016.04.131

[25] Khamlaj, Tariq Abdulsalam, and Markus Peer Rumpfkeil. "Analysis and optimization of ducted wind turbines." *Energy* 162 (2018): 1234-1252. https://doi.org/10.1016/j.energy.2018.08.106

[26] Y. Y. Maw and M. T. Tun, "sensitivity analysis of angle, length and brim height of the diffuser for the small diffuser augmented wind turbine using the numerical investigation," *asean engineering journal* 11, no. 4 (2021): 280-291. https://doi.org/10.11113/aej.v11.18102

[27] Aravindhan, N., M. P. Natarajan, S. Ponnuvel, and P. K. Devan. "Recent developments and issues of small-scale wind turbines in urban residential buildings-A review." *Energy & Environment* 34, no. 4 (2023): 1142-1169. https://doi.org/10.1177/0958305X221084038

[28] Elsayed, Ahmed M. "Design optimization of diffuser augmented wind turbine." *CFD Letters* 13, no. 8 (2021): 45-59. https://doi.org/10.37934/cfdl.13.8.4559

[29] Fletcher, Roger. *Practical methods of optimization*. John Wiley & Sons, 2000. https://doi.org/10.1002/9781118723203

[30] Long, Qiang, Changzhi Wu, Xiangyu Wang, Lin Jiang, and Jueyou Li. "A multiobjective genetic algorithm based on a discrete selection procedure." *Mathematical Problems in Engineering* 2015 (2015). https://doi.org/10.1155/2015/349781

[31] Poles, Silvia. "MOGA-II an improved multi-objective genetic algorithm." *Estecotechnical Report* 6 (2003).

[32] Reeves, Colin, and Jonathan E. Rowe. *Genetic algorithms: principles and perspectives: a guide to GA theory*. Vol. 20. Springer Science & Business Media, 2002. https://doi.org/10.1007/b101880